Proceedings of ESDA2004
7th Biennial ASME Conference on Engineering Systems Design and Analysis
July 19-22, 2004, Manchester, UK

ESDA2004-58396

VISUALISATION OF TWO-PHASE GAS-LIQUID PIPE FLOWS USING ELECTRICAL CAPACITANCE TOMOGRAPHY

Andy Hunt
Tomoflow Ltd, Dorchester, United Kingdom
ahunt@tomoflow.com

John Pendleton
Tomoflow Ltd, Dorchester, United Kingdom
jpendleton@tomoflow.com

Yves Ladam
SINTEF Petroleum Research, Trondheim, Norway
Yves.Ladam@iku.sintef.no

Keywords: electrical capacitance tomography, ECT, multiphase flow, slug flow, flow visualization.

ABSTRACT

Electrical Capacitance Tomography (ECT) has been used over a number of years to measure concentration distribution, and more recently velocity distribution, in two-phase flows. ECT is non-intrusive, and the reconstruction of the concentration and velocity distribution can be undertaken in real time and over an arbitrary number of zones in the flow cross-section. In this paper the concept of a 'virtual instrument' is introduced where zones of the image can be structured for comparison with other measurements. Numerical agreement with gamma-ray density measurements is shown to be excellent in slug and stratified flows.

We present a series of measurements undertaken in complex oil/gas slug flows in a large flow loop. We present a variety of 2-D cross-sectional images, time series velocity and concentration graphs and 3-D contour plots. The good temporal and spatial resolution of ECT throws an extensive new light on these otherwise difficult to measure dynamic flow structures. In particular with bubbly-slug structures known as 'ghosts' ECT shows clearly that they are in fact bubbly waves which have extended 'wings' up and around the pipe.

INTRODUCTION

Electrical capacitance tomography is one of the imaging techniques most likely to provide quantitative flow visualization and flowrate information in industrial flows. It has particular advantages in two-phase oil/gas flows typical of those in the petroleum industry [1], [2] and is also widely applicable in gas/solids flows [3], [4], [5].

Previous authors have presented cross-sectional concentration images of multiphase flows (eg [1], [3], [4]) and estimates of velocity and volumetric flowrates [4], [5], [6]. These latter estimates have been compared numerically with integrated flows over time, but no detailed comparisons with other real-time local measurements have been published for two-phase oil/gas slug flows.

This paper presents results taken during 2003 using ECT in the multiphase flow loop at SINTEF in Norway (Figure 1). We focus here on the numerical comparison with a gamma-ray densitometer which was placed adjacent to the ECT system in the flow loop.

ELECTRICAL CAPACITANCE TOMOGRAPHY

ECT measurements are made by placing rings of electrodes around the circumference of the pipe or vessel of interest, measuring the electrical capacitance between each independent pairing of electrodes and using image reconstruction techniques to show the permittivity distribution within the sensor. Figure 2 shows a typical 8-electrode array, while Figure 3 shows a typical cross-sectional image. The vertical bar on the left hand side of the figure shows the concentration scale from red (100% oil, 0% air) to blue (0% oil, 100% oil). The vertical bar on the right hand side of the figure shows graphically the average concentration across the whole plane. The 'volume fraction' figure shown is another way of stating average concentration and is directly equivalent.

In our experiments we used a Tomoflow R100 ECT Flow Analysis System with a twin-plane 8 segment guarded array of electrodes, where the electrode axial length was 30mm. The planes are separated by 100mm axially and the acquisition rate was 200 frames per second on both planes – the fastest rate currently available on a commercial ECT system [7].

The use of capacitance measurement for volume fraction estimation in non-conducting two-phase flows is well known, but the measurements are strongly dependent on sensor

geometry and flow regime [8]. ECT offers an important improvement in that it measures the full concentration distribution in any regime or geometry.

ECT generates large quantities of information: concentration in two planes (over 800 pixels in each) several hundred times per second, and we calculate velocities over several zones (up to 10 or more) at each time step. Interpreting, analyzing and presenting this data can be done in many ways, and we are at the early stages of learning how best to do this for different applications.

EXPERIMENTAL FACILITY

The flow facility is a 217m long horizontal loop around which a variety of fluids may be pumped and which is very flexible in operation. Most of the rig is steel 0.069m inner diameter but some transparent PVC sections are inserted for observations. The mixture of fluids may contain water, oil and either air or sulphur hexafluoride gas (SF_6). A 25m section dedicated to sand transport can also be inserted. The maximum operating pressure is 10bar, and the superficial velocity for the liquids range from 0.003m/s to 2m/s with 0.5m/s to 15m/s for the gas. (note: superficial velocity is the volumetric flowrate of the individual phase divided by pipe cross-sectional area)

For this particularly project the fluids used were Exssol d80 and air at atmospheric pressure, the physical parameters of the fluids are given in Table 1.

Measurements were performed in a 25m long section of transparent tubing within a shelter about 40m from the end of the loop where the fluids are separated. The first 150m are considered as inlet section to allow the flow to develop.

REFERENCE INSTRUMENTATION

The superficial velocities of the experimental fluids were measured in single phase lines before the mixing point at the start of the loop. Liquid flow rate is measured by coriolis meter (uncertainty 0.1% of full-scale), gas flow rate is measured by vortex meter (uncertainty 1% of full-scale). A single-beam gamma-ray densitometer was placed adjacent to the ECT sensor. Such single-beam gamma meters are well studied in two-phase gas-liquid flows, and known to give reliable measurements of equivalent liquid height in stratified flows [9], [10]. In addition video recording of the flow patterns through the transparent pipe wall was undertaken and absolute pressure and pressure gradient were measured in the test section.

FLOW CONDITIONS

Oil and air flows were used with superficial gas velocities of between 0.2 and 12m/s and superficial oil velocities of 0.05 to 1.0m/s. Gas concentrations (void fraction) ranged from 6% to 55%. Flow conditions varied from stratified flow where the two phases flow smoothly in separate parts of the pipe, through slug flow with long coherent fluid slugs to highly turbulent periodic passage of frothy flow structures (known colloquially as 'ghosts').

In a typical horizontal gas-liquid flow at these velocities flow the dominant structure is the slug, whose passing frequency and turbulence intensity increases as the flow velocity increases. Figure 4 shows a video frame of the arrival of an oil slug (yellow), Figure 5 a slug tail, and Figure 6 the stratified flow between slugs. The image in Figure 3 corresponds approximately to the cross-section at the centre of Figure 4.

FLOW ANALYSIS FROM IMAGES

Twin-plane sensors were used in conjunction with guard electrodes to create two image 'planes' axially separated along the flow. Each 'plane' (as shown in Figure 3) is in fact a cylinder of 30mm length made up of 812 pixels on a 32x32 square. To investigate details of flow conditions it is often more helpful to divide each image plane into a number of zones arranged appropriately for the flow conditions. For flow measurement purposes it is often useful to divide the flow into equal-sized zones, but here, to facilitate comparisons with the reference gamma-ray densitometer, we define a 'virtual instrument' from the image to mimic the spatial sensitivity of the gamma-ray meter. The 'virtual instrument' zone is a simple double line of pixels arranged vertically across the flow, as shown in Figure 7. The central zone contains 64 out of the 812 total pixels. The concentration value within each zone can now be expressed against time as the arithmetic average of all the pixel values within the zone.

COMPARISON OF ECT WITH GAMMA-RAY DENSITY

Figure 8 shows concentration data from our experiments. The left hand axis applies to the ECT measurement of concentration averaged over the 'virtual instrument' zone. The plain red line shows the concentration estimated from plane 2 of the twin-plane ECT system (the upstream plane), while the dotted green line shows plane 1 (downstream). The horizontal axis shows time in seconds, a total of about 8 seconds of data.

It can be seen from Figure 8 that concentration varies periodically with time as each slug passes, and 6 slugs pass within the 8 seconds shown. The periods of high concentration – approximately 90% liquid – are the liquid slugs, while in between are lengths of stratified flow – 30% to 40% liquid. The stratified portions show steady drainage of height before the arrival of the next slug. The right hand axis in the figure shows the gamma-ray density 'liquid-height' to the same scale as the ECT 'virtual instrument' concentration.

Figure 9 shows a shorter section of the same data as Figure 8 to allow the small differences between the measurements to be seen more clearly. Comparison with the gamma-ray measurements show good agreement in the stratified and slug flow periods. The time separation between the two planes of the ECT system is used to estimate the velocity of transit (see next section), but the gamma-ray output has been time shifted to match the ECT timing with the devices separated by 0.4m along the pipe. Differences between the ECT and gamma-ray estimates may be due to instrument errors, or evolution of flow structures along the pipe. In practice it appears that the high frequency oscillation of the gamma-ray signal is due to statistical noise, and other differences are so small that it is clear that these particular flow structures do not evolve significantly at this separation. Since the loop is 217m long and all the measurements presented here are made within about 0.5 m, this latter conclusion is perhaps not surprising.

In principle the gamma-ray calibration is only valid for flows which are horizontally stratified, but in the flows shown here this is not a serious limitation. In vertical and deviated pipes the limitation is much more severe and future papers will investigate these errors. The gamma-ray has a longer averaging

time (0.02s for the gamma ray compared with 0.005s for ECT) and other experiments show that the differences between the measurements appear to be in the favour of ECT in fast highly structured flows.

FLOW VELOCITIES

The velocity at each point in time within each zone is calculated by correlating the instantaneous concentration of one plane with the same zone in the other plane. Reference [5] describes this process in detail. Although mathematically the correlation is described for the averaging time approaching infinity, in practice the velocity will fluctuate over some much shorter time scale and the user will need to set the averaging window at some suitable value appropriate to the particular length and velocity scales in the flow and the sensor geometry.

The correlogram has a clearly discernible peak if the flow structures are coherent over the sensor length and contains information about the time domain statistics of the flow – primarily convection and dispersion. The simplest assumption is that the time delay at the peak of the correlogram corresponds to the transit time of flow structures between the two planes. This does not assume that the flow structures do not evolve, it is simply an estimate of the axial velocity component. For other applications the dispersion may be modeled [11] or other velocity components may be measured [12]. The correlogram peak may be found by the greatest single value, centre of area or polynomial fitting. For many flows polynomial fitting gives the most consistent results though all the other techniques are available in our software. The time window used for the correlation process needs to be shaped in some way to minimize artefacts caused by sharp-edged windows. This shaping is known as apodization – the results presented here use the common Hanning window, which is a smooth bell shape.

Figure 10 shows the same slug flow data as Figures 8 and 9, but this time the right hand axis shows the velocity of transit between the two planes, as estimated from the correlation between two concentration signals. As obvious from visual observations, the slug velocity does not vary greatly from slug to slug. In this case the velocity is between 2.5 and 3.5 m/s.

3-D IMAGES

By plotting 3-dimensional pictures based on the images as time slices separated by the local transit time we can generate concentration contours that clearly show the internal structure of the flows. Other workers have plotted 3-D pictures through simple stacking of images based on the sampling time, for example [13], but our images space the planes based on measured transit velocity. Direct 3-D imaging may be possible in the future [14]. Images such as we present here show the structure as it passes a fixed point, possibly at varying velocity, and if the structures are not rapidly evolving in time this is almost equivalent to a 'snapshot' of the structure.

It is apparent from the images that many of the 'slug' structures have an air-core passing through the centre. One particular type of bubbly slug is known colloquially in Norwegian as a 'ghost' because it drifts past in the working section with a particular soft whispering sound. Figure 11 shows the 50% concentration contour for one of these structures. Note that in the figure the axis along the flow direction has been significantly compressed with respect to the radial axis. From the outside of the pipe these ghosts appear as frothy slugs with no particular structure visible. Seen from ECT measurements however it is apparent that they are bubbly waves which have thrown 'wings' up around the pipe circumference leaving an air core.

Such structural visualizations are limited by the fact that the 50% contour is not actually an interface, but they give an unusually good insight into the way the flows are built. It should also be remembered that the pictures are a way of presenting quantitative data, and not just qualitative indications. Within each pixel we have a numerical measurement of concentration at every point in time and within each zone a good estimate of axial velocity.

CONCLUSIONS

ECT is an established method of visualizing the cross-sectional permittivity distribution in non-conducting flows. We have extended the analysis of the images to allow the calculation of velocity distribution across user-defined zones representative of the flow scale. For complex oil/gas slug flows we have presented a variety of 2-D cross-sectional images, time series velocity and concentration graphs and 3-D contour plots.

Direct comparisons with gamma-ray density measurements have been made through the introduction of a 'virtual instrument' using the ECT images to mimic the spatial sensitivity of the gamma ray system. Quantitative agreement between the two techniques is excellent in stratified and coherent slug flow.

The good temporal and spatial resolution of ECT throws an extensive new light on the complex flows in horizontal gas-liquid systems. Such dynamic flow structures are otherwise difficult to measure quantitatively. In particular, a type of structure known as a 'ghost', which appears visually from outside the pipe to be a bubbly slug is shown by ECT to be a bubbly wave which has extended 'wings' up and around the pipe.

ECT gives a full 3D picture of the multiphase flow structures. Within each pixel there is a numerical measurement of concentration at every point in time and within each zone a good estimate of axial velocity.

ACKNOWLEDGMENTS

We are grateful to the Commission of the European Community for funding the flow loop time at SINTEF under the SIMLAB project. We would also like to thank staff at the SINTEF three-phase flow laboratory for their cheerful help in performing the experiments described. We acknowledge the support of the UK DTI through a SMART feasibility award to Tomoflow Ltd.

REFERENCES

[1] Thorn R., Huang S.M., Xie C.G., Salkeld J.A., Hunt A., and Beck M.S. (1990) Flow imaging for multi-component flow measurement. Flow Meas. Instr. 2, Oct 1990.

[2] Thorn R., Johansen G.A. and Hammer E.A. 1999. Three-phase flow measurement in the offshore oil industry – is there a place for process tomography? 1st World Congress on Industrial Process Tomography, Buxton, UK, 14-17 April 1999.

[3] Hunt A., Pendleton J.D., and White RB, 2003. A Novel Tomographic Flow Analysis System. 3rd World Congress

on Industrial Process Tomography, Banff, Canada, 3-5 September 2003.
[4] Jaworski A.J. and Dyakowski T. 2001. Tomographic measurements of solids mass flow in dense pneumatic conveying. What do we need to know about the flow phyics? 2nd World Congress on Industrial Process Tomography, Hannover, Germany, 29-31 August 2001.
[5] Hunt A., Pendleton J.D. and Byars M. 2004. Non-intrusive Measurement of Volume and Mass using Electrical Capacitance Tomography. ESDA2004-58398.
[6] Fehmers G. 2003. Volumetric flowrates from Impedance Tomography in oil/gas flows. 3rd World Congress on Industrial Process Tomography, Banff, Canada, 3-5 September 2003.
[7] Byars M. and Pendleton J.D. 2003, A new high-speed control interface for an electrical capacitance tomography system, 3rd World Congress on Industrial Process Tomography, Banff, Canada.
[8] Lucas G.P. 1987, The measurement of two-phase flow parameters in vertical and inclined flows, PhD Thesis, University of Manchester Institute of Science and Technology (UMIST), UK.
[9] Chan A.M.C. and Barnerjee S. 1981, Design aspects of gamma densitometers for void fraction measurements in small scale two phase flows. Nuclear Instruments and Methods vol 190 pp135-148.
[10] Linga H. 1991, Measurements of two phase flow details. Non intrusive methods applied to slug and dispersed flows. PhD thesis Trondheim University.
[11] Fuchs A. and Brandstätter B. 2003, Development of a signal prediction based ECT-system for precise flow velocity measurement. 3rd World Congress on Industrial Process Tomography, Banff, Canada.
[12] Mosorov V., Sankowski D., Mazurkiewicz L. and Dyakowski T. 2002, The 'best-correlated pixels' method for solid mass flow measurements using electrical capacitance tomography, Meas. Sci. Technol. 13 1810-1814.
[13] Wang H., Liu S., Jiang F. and Yang W. 2003, 3D presentation of images with capacitance tomography. 3rd World Congress on Industrial Process Tomography, Banff, Canada.
[14] Warsito W. and Fan L.-S. 2003, Development of 3-dimensional electrical capacitance tomography based on neural network multi-criterion optimization. 3rd World Congress on Industrial Process Tomography, Banff, Canada.

TABLES

	Density	Visvosity
Air	1.2 kg/m3	0.015 mPa.s
Exssol d80	795 kg/m3	2mPa.s

Table1: fluids properties

FIGURES

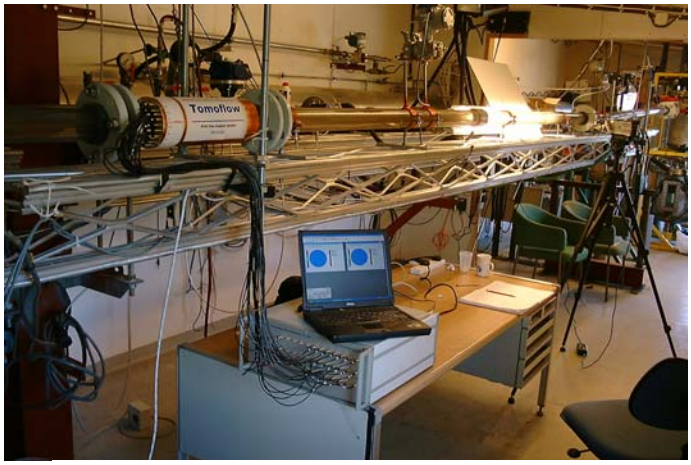

Figure 1. Upper: photograph of test section (flow moving away from camera), lower: flow loop layout

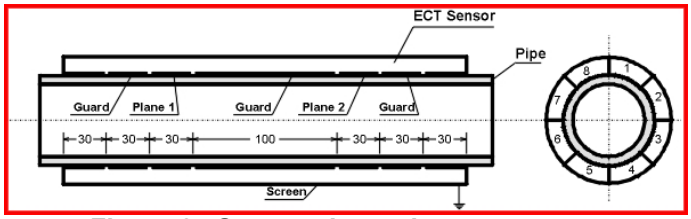

Figure 2. Sensor electrode arrangement

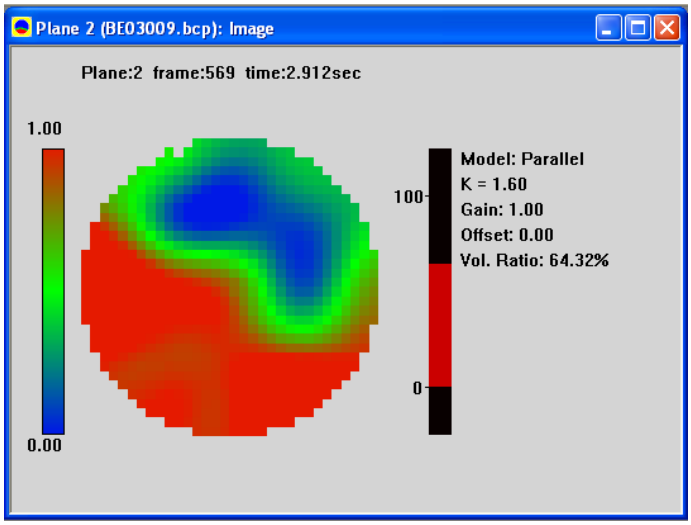

Figure 3. ECT image of gas-liquid slug cross-section.

Figure 4. Photograph of slug front (flow left to right).

Figure 5. Photograph of slug tail (flow left to right).

Figure 6. Stratified flow (flow left to right).

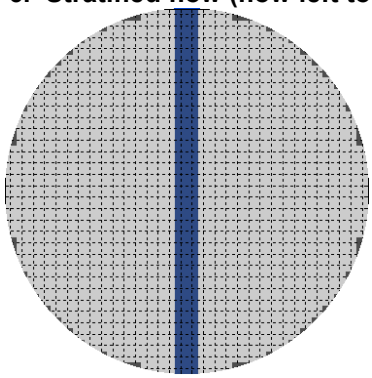

Figure 7. 'Virtual instrument' zone for comparison with gamma-ray density measurement.

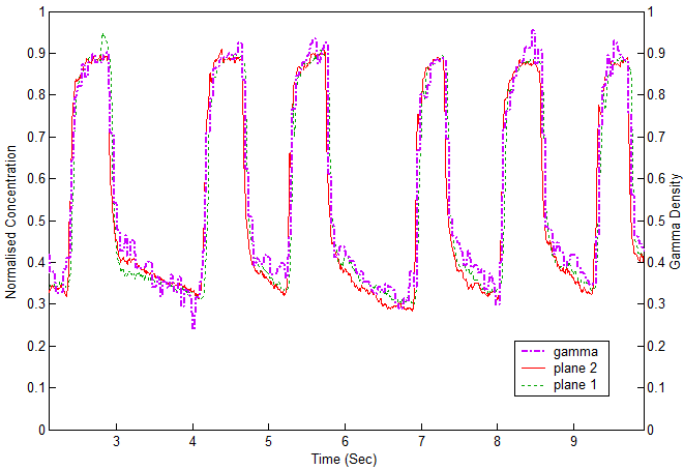

Figure 8. Comparison of twin-plane ECT concentration measurement with line-average gamma-ray density estimate of concentration.

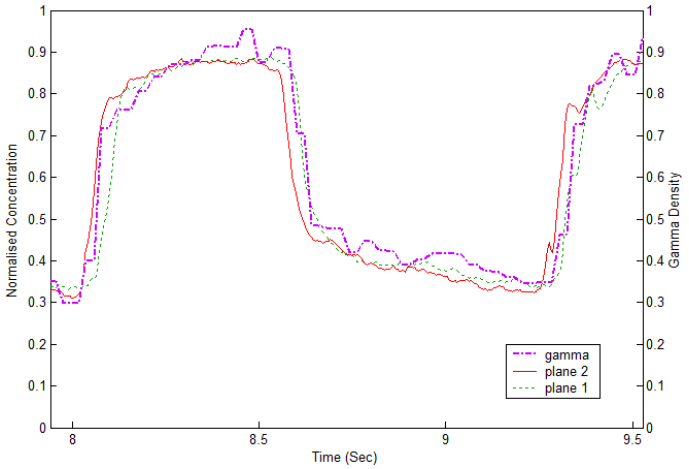

Figure 9. Part figure 8, with expanded time scale.

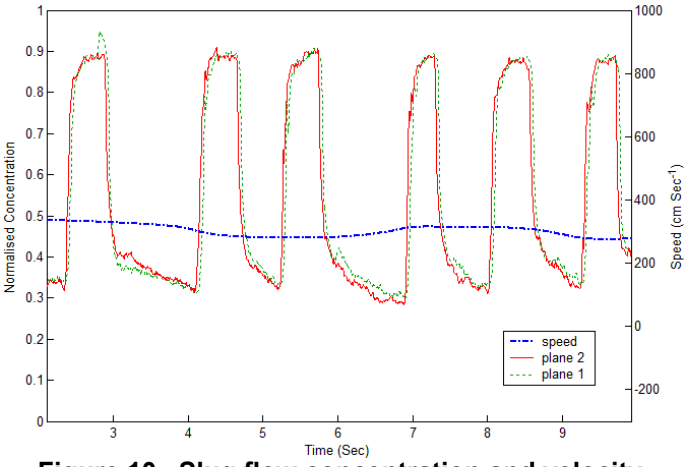

Figure 10. Slug flow concentration and velocity.

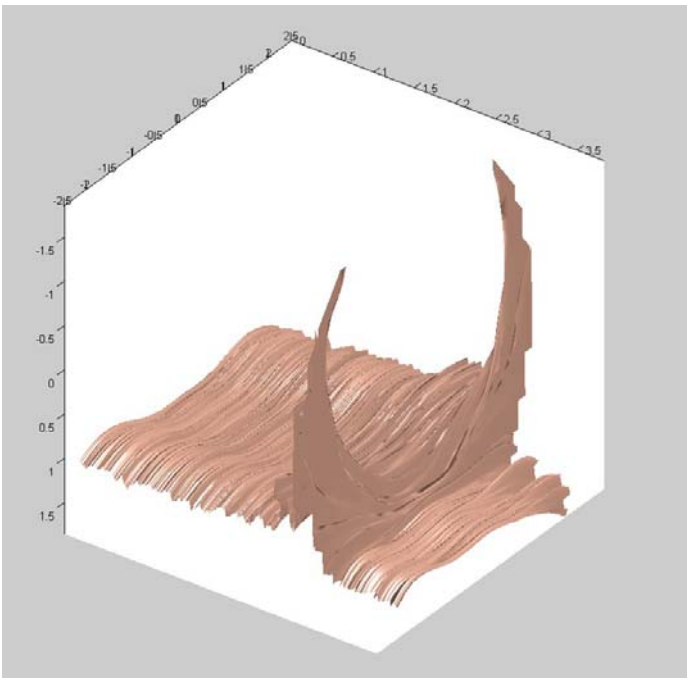

Figure 11. 3-D surface at 50% concentration – 'ghost'. Pipe not shown. Radial scale expanded.